# Infrared Spectra and Theoretical Calculations for Fe, Ru, and Os Metal Hydrides and Dihydrogen Complexes

**Xuefeng Wang and Lester Andrews***

*Department of Chemistry, P.O. Box 400319, University of Virginia, Charlottesville, Virginia 22904-4319*

*Received: July 31, 2008; Revised Manuscript Received: November 13, 2008*

Laser-ablated iron, ruthenium, and osmium atoms react with hydrogen in excess argon, neon and pure hydrogen to produce the $FeH_2$ molecule, and the $FeH_2(H_2)_3$, $RuH(H_2)_4$, $RuH_2(H_2)_4$, and $(H_2)MH$ complexes (M = Fe, Ru, Os), as identified through infrared spectra with $D_2$ and HD substitution. DFT frequency calculations support the assignment of absorptions observed experimentally. The $FeH_2$ molecule has a quintet ground state with a quasi-linear structure, and is repulsive to the addition of one more $H_2$ ligand: however, with three more $H_2$ ligands, stable triplet and singlet state $FeH_2(H_2)_3$ supercomplexes can be formed. The quintet $FeH_2$ molecule and $FeH_2(H_2)_3$ supercomplex undergo reversible near-ultraviolet photochemical rearrangement in solid neon and hydrogen. The $RuH_2$ molecule has a bent triplet ground state and forms the stable singlet $RuH_2(H_2)_4$ supercomplex, but only the latter is observed in these experiments. In like fashion RuH has a quartet ground state and the doublet $RuH(H_2)_4$ complex is trapped in solid hydrogen. All three $(H_2)MH$ complexes with lower energy than $MH_3$ are trapped, and no absorptions are observed for $MH_3$ molecules.

## Introduction

Group 8 metal hydrides have sustained interest because they are important in catalytic processes such as hydrogenation, alkane activation, and astrophysics.[1−5] The mononuclear iron center in hydrogenase metalloenzymes is particularly effective for activating hydrogen molecules.[6] The diatomic FeH molecule with $^4\Delta$ ground state and 1758.7 $cm^{-1}$ vibrational fundamental has been characterized in the gas phase.[7] The photochemical reaction of Fe + $H_2$ was investigated earlier by Ozin and McCaffrey in solid xenon,[8] and by Rubinovitz and Nixon in solid krypton and argon.[9] Later studies employed laser-ablated Fe atoms, and infrared spectra of FeH and $FeH_2$ in solid argon were reported by this group.[10] The $FeH_2$ molecule was found to be linear or quasi-linear and to favor the high spin $^5\Delta$ ground state by LMR spectroscopy in the gas phase, which is in very good agreement with theoretical calculations.[11,12] Subsequent CCSD(T) theoretical work on the $FeH_3$ molecule finds a high spin ground state with a much higher diagnostic frequency.[13] Although stable binary iron dihydride complexes with dihydrogen have not been prepared, ligand stabilized organometallic $FeH_2(H_2)L_3$ derivatives have been thoroughly investigated.[14]

Simple binary ruthenium and osmium hydride molecules are unknown, but the ternary metal hydride $Na_3RuH_7$ has been synthesized by the reaction of alkali metal hydrides with ruthenium under hydrogen pressure.[15] Laser-ablated ruthenium atom reactions with $H_2$ and CO mixtures provided ruthenium carbonyl hydrides, $H_2Ru(CO)_x$ ($x$ = 2−4) and the complex $(H_2)RuCO$.[16] A large variety of neutral ligand stabilized $RuH_2$ and $OsH_2$ $\eta^2$-dihydrogen complexes have been synthesized,[17,18] and catalytic hydrogenation and carbon−carbon bond activation by ruthenium hydride complexes have been investigated extensively.[19−23]

Molecular hydrogen has been used as both reagent and matrix in laser-ablated metal atom reactions with hydrogen in this laboratory. Laser-ablated metal atoms react with hydrogen upon co-condensation in pure $H_2$ and give abundant metal hydrides and hydrogen complexes. For example, dialane $H_2Al(\eta^2\text{-}H_2)AlH_2$ was successfully synthesized for the first time with this method, and the metal polyhydrides $(H_2)_2CrH_2$, $(H_2)MH$ (M = Cu, Ag, Au), $AuH_4^-$, $MH_4$ (M = Sn, Pb), and $MH_4(H_2)_4$ (M = W, Th) have been identified.[24−27]

We report here the reactions of laser-ablated Fe, Ru and Os atoms with $H_2$ in pure $H_2$ and solid neon and argon matrixes. Binary iron, ruthenium, and osmium hydrides and dihydrogen complexes were identified through matrix isotopic infrared spectra, comparison of different matrix shifts, and quantum chemical calculations. A preliminary communication on the $RuH_2(H_2)_4$ complex in solid hydrogen has appeared.[28]

## Experimental and Computational Methods

The experiment for reactions of laser-ablated metal atoms with hydrogen has been described in detail previously.[29] The Nd:YAG laser fundamental (1064 nm, 10 Hz repetition rate with 10 ns pulse width) was focused onto a rotating high-purity iron (Johnson Matthey), ruthenium or osmium target (Metallium, Inc.). The laser energy was varied from 10 to 20 mJ/pulse. Laser ablated metal atoms were codeposited with pure hydrogen or hydrogen (1 to 4%) in excess neon onto a 4 K CsI cryogenic window at 2−4 mmol/hour for one hour. Isotopic $D_2$ and HD (Cambridge Isotopic Laboratories) and selected mixtures were used in different experiments. FTIR spectra were recorded at 0.5 $cm^{-1}$ resolution on Nicolet 750 with 0.1 $cm^{-1}$ frequency accuracy using an Hg−Cd−Te range B detector. Matrix samples were annealed at different temperatures, and selected samples were subjected to broadband photolysis by a medium pressure mercury arc lamp (Philips, 175 W) with globe removed.

DFT (density functional theory) calculations of metal hydrides and hydrogen complexes were done following previous works.[24−29] The Gaussian 03 program[30] was employed to calculate the structures and frequencies of expected molecules. The 6-311+G(3df,3pd) basis set for H and Fe atoms and SDD pseudopotentials for ruthenium and osmium atoms were used.[31,32] All the geometrical parameters were fully optimized with the

* Corresponding author. E-mail: lsa@virginia.edu.

10.1021/jp806845h CCC: $40.75 
Published on Web 12/18/2008

**TABLE 1: Infrared Absorptions ($cm^{-1}$) Observed from Reaction of Iron and Dihydrogen in Argon, Pure Hydrogen, and Neon Matrixes**

| argon | | | hydrogen | | | neon | | | |
|---|---|---|---|---|---|---|---|---|---|
| $H_2$ | HD | $D_2$ | $H_2$ | HD | $D_2$ | $H_2$ | HD | $D_2$ | ident |
| | | | 1913.5 | | | 1921.2 | | | $FeH_2(H_2)_3$ |
| | | | | | 1389.8 | | | 1394.3 | $FeD_2(D_2)_3$ |
| | | | 1830.4 | 1834.4 | | 1839.3 | 1839.2 | | $FeH_2(H_2)_3$ |
| | | | | | 1331.5 | | | 1335.9 | $FeD_2(D_2)_3$ |
| | | | 1713.6 | 1715.9 | | 1728.7 | 1726.5 | | $(H_2)_xFeH$ |
| | | | 1704.7 | 2706.2 | | | | | $(H_2)_xFeH$ |
| | | | 1698.5 | 1698.5 | | | | | $(H_2)_xFeH$ |
| 1766.4 | | | | | | | | | (argon)FeH |
| | | | | 1235.7 | | | 1229.2 | 1228.6 | $(D_2)_xFeD$ |
| | | | | 1229.6 | | | | | $(D_2)_xFeD$ |
| | | | | 1223.1 | 1222.3 | | | | $(D_2)_xFeD$ |
| | | 1277.0 | | | | | | | (argon)FeD |
| | | | | | | 1680.9, | 1708.8 | | $FeH_2$ (site) |
| | | | | | | 1679.0, | 1704.8 | | $FeH_2$ (site) |
| 1660.6 | | | 1666.4 | 1665.2 | | 1674.6 | | | $FeH_2$ |
| | 1690.3, | | | 1693.5, | | | 1697.1 | | FeHD |
| | 1215.2 | | | 1218.2 | | | 1220.8 | | |
| | | | | | | | 1225.5 | 1218.6, | $FeD_2$ (site) |
| | | | | | | | 1223.7 | 1214.1, | $FeD_2$ (site) |
| | | 1204.2 | | 1207.7 | 1205.7 | | 1220.8 | 1210.0 | $FeD_2$ |
| | | | 1088 | | | | | | $FeH_2(H_2)_3$ |
| | | | 1056 | | | | | | $FeH_2(H_2)_3$ |
| | | | 633.0 | 534.9 | | 627.1 | 518.7 | | $FeH_2(H_2)_3$ |
| | | | | 519.6 | 473.2 | | 508.8 | 472.8 | $FeD_2(D_2)_3$ |

B3LYP functional.[33] Complementary calculations were done with the BPW91 functional and the MP2 method.[30,34] Analytical vibrational frequencies were obtained at the optimized structures.

## Results

Infrared spectra collected from Fe, Ru, and Os atom reactions with hydrogen in pure $H_2$, $D_2$, $H_2 + D_2$, and HD codeposited at 4 K will be presented. The spectra from reactions in excess neon and argon are also described for comparison. In addition DFT calculations were performed to support the product identifications.

**Iron.** Laser-ablated iron atoms were codeposited with molecular hydrogen, and product absorptions are listed in Table 1. Argon matrix experiments were repeated using lower laser energy, and infrared spectra were essentially the same as reported previously.[10] In pure hydrogen, a strong band at 1666.4 $cm^{-1}$, a trio of bands at 1698.4, 1704.6, 1713.8 $cm^{-1}$, and weak bands at 1830.4 and 1912.5 $cm^{-1}$ were observed in the Fe−H stretching region after deposition as shown in Figure 1. Additional bands were observed at 1088, 1056, and 633.0 $cm^{-1}$, which are shown in Figure 2. Annealing to 6 K reduced the strong band and increased the weaker, higher frequency bands and the 1088, 1056, and 633.0 $cm^{-1}$ bands. Subsequent 240−380 nm irradiation restored part of the strong absorption and slightly increased the weaker bands. In a second experiment, irradiation >470 and >380 nm decreased the major band and slightly increased the two higher bands, but with >220 nm broadband irradiation, this photochemistry reversed. In a third experiment >290 and >220 nm irradiation cycles, shown in Figure 2, decreased the 1666.4 $cm^{-1}$ band but increased the 1830.4, 1912.5, 1088, 1056, and 633.0 $cm^{-1}$ absorptions and reversed them in concert. With pure $D_2$ a very sharp and strong band at 1205.7 $cm^{-1}$ and weak bands at 473.2, 1222.3, 1331.5 and 1389.8 $cm^{-1}$ are the Fe−D counterparts of the stronger new products in hydrogen experiments. The HD experiment (Figure 1, this experiment employed lower laser energy to minimize isotopic exchange and thus produced a lower initial product yield than the pure $H_2$ and pure $D_2$ reactions) gave an absorption pair at 1693.5 and 1665.2 $cm^{-1}$, and trio at 1715.9, 1706.2, 1698.5 $cm^{-1}$ and a single band at 1834.4 $cm^{-1}$ in the Fe−H stretching region, and a pair at 1218.2 and 1207.7 $cm^{-1}$, and trio at 1235.7, 1229.6, and 1223.1 $cm^{-1}$ in the Fe−D stretching region. An $H_2 + D_2$ mixture gave the same strong absorptions as the pure isotopic reactions, but slightly shifted owing to the different

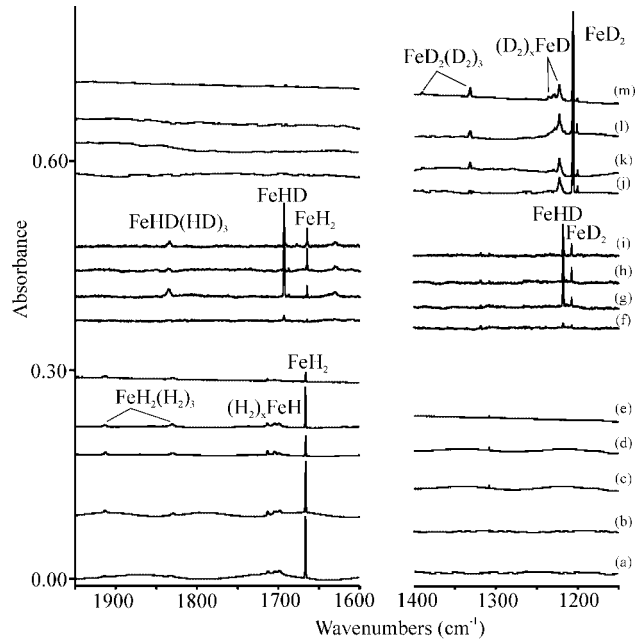


**Figure 1.** Infrared spectra for the iron atom and $H_2$ reaction products in pure $H_2$ at 4.5 K: (a) Fe + $H_2$ deposition for 30 min, (b) after annealing to 6 K, (c) after annealing to 6.5 K, (d) after 240−380 nm irradiation, (e) after annealing to 6.5 K, (f) Fe + HD deposition for 30 min using lower laser energy, (g) after >320 nm irradiation, (h) after full-arc irradiation, (i) after annealing to 8 K, (j) Fe + $D_2$ deposition for 30 min, (k) after annealing to 7.5 K, (l) after >220 nm irradiation, (m) after annealing to 10 K.

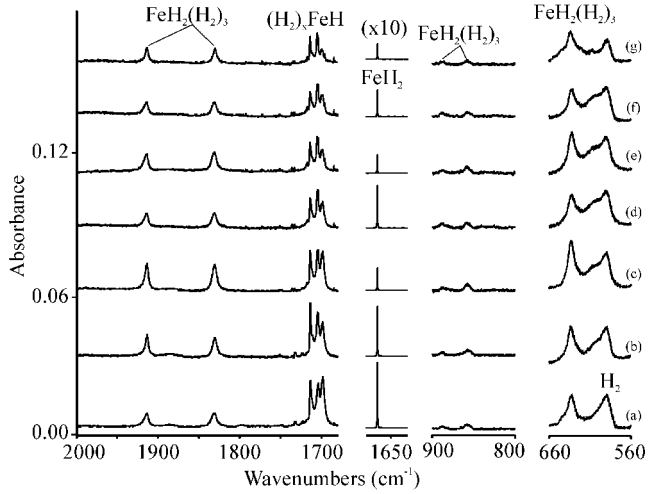


**Figure 2.** Infrared spectra for the iron atom and $H_2$ reaction products in pure $H_2$ at 4.5 K: (a) Fe + $H_2$ deposition for 30 min, (b) after annealing to 6 K, (c) after >290 nm irradiation, (d) after >220 nm irradiation, (e) after >290 nm irradiation, (f) after >220 nm irradiation, (g) after annealing to 6.3 K. The absorbance scale for the 1600 $cm^{-1}$ region is 10 times higher than indicated.

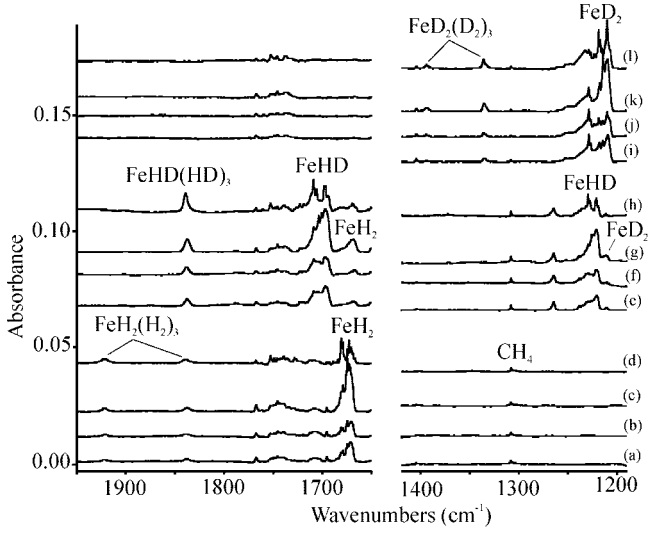


**Figure 3.** Infrared spectra for the iron atom and $H_2$ reaction products in neon at 4.5 K: (a) Fe + $H_2$ (2%) deposition for 60 min, (b) after annealing to 7 K, (c) after >220 nm irradiation, (d) after annealing to 11 K, (e) Fe + HD (2.5%) deposition for 60 min, (f) after annealing to 7 K, (g) after full-arc irradiation, (h) after annealing to 11 K, (i) Fe + $D_2$ (2%) deposition for 60 min, (j) after annealing to 8 K, (k) after >290 nm irradiation, (l) after annealing to 11 K.

medium, and a single band at 1834.1 $cm^{-1}$. Pure hydrogen matrix experiments provide a reducing atmosphere, and the weak iron oxide absorptions, typically observed in solid argon,[35] are not observed in solid hydrogen. Experiments in solid neon (Figure 3) gave similar spectra as in pure hydrogen, but the bands exhibited splitting, and the product absorptions are listed in Table 1.

**Ruthenium.** Reactions of ruthenium atoms with $H_2$ in excess argon produced only one weak new band, at 1821.0 $cm^{-1}$, with $D_2$ counterpart at 1312.2 $cm^{-1}$, which were reported in our earlier investigation.[16] Atoms of Ru in solid $H_2$ produced new bands at 2690 $cm^{-1}$ in the H−H stretching region, at 2003.3 and 1983.9 $cm^{-1}$ in the terminal Ru−H stretching region, at 1857.1, 1850.1, 1540.6, and 873.9 $cm^{-1}$ in the Ru−($H_2$) stretching region, and at 773.8, 771, 708.5, and 588.2 $cm^{-1}$ in the Ru−$H_2$ bending and deformation region, which are labeled A in Figure 4. The weaker group labeled B at 1947.5, 1729.5, 833.1, 675.6, 567.6, and 549.0 $cm^{-1}$ decreased on UV irradiation and restored in part on annealing. Para-hydrogen gave almost the same spectrum, as shown at the top of Figure 4. Figure 5 shows more detail in the upper region. Deuterium counterparts in pure $D_2$ were observed at 1994, 1978, 1445.2, 1428.3, 1403.8, 1337.9, 1330.8, 652.2, and 555.6 $cm^{-1}$. It was found that these absorptions are barely affected by irradiation. With pure HD several new bands were observed as listed in Table 2. Again, the pure hydrogen experiments were free of oxide absorptions.[36] In solid neon two strong bands at 2003.5 and 1983.9 $cm^{-1}$ for Ru + $H_2$ reactions and 1442.5 and 1425.6 $cm^{-1}$ for Ru + $D_2$ reactions are the major product absorptions (Figure 6). Weak associated bands are given in Table 2.

**Osmium.** Osmium atom reactions with hydrogen in excess argon produced new absorptions at 1873.6, 1935.1, 1963.4, and 1994.9 $cm^{-1}$, which are listed in Table 3 and illustrated in Figure 7. Irradiation >380 nm decreased these bands, but annealing to 25 K restored them. The osmium reaction in pure hydrogen gave two weak bands at 1993.8 and 1962.1 $cm^{-1}$ and a strong band at 1930.6 $cm^{-1}$. On annealing and irradiation, the 1993.8 $cm^{-1}$ band decreased while the 1962.1 and 1930.6 $cm^{-1}$ bands increased. In pure $D_2$ these bands shifted to 1431.2, 1421.1, and 1391.0 $cm^{-1}$, respectively, as compared in Figure 8. Experiments with pure HD gave new absorptions at 1993.8, 1930.4 and 1433.1 $cm^{-1}$. Osmium atom reactions with $H_2$ in solid neon are very similar (Figure 9), and absorptions for reaction products are listed in Table 3.

**Calculations.** DFT calculations are done for iron, ruthenium, and osmium hydrides and their dihydrogen complexes, and the results are listed in Tables 4, 5 and 6. The ground state of FeH is found to be $^4\Delta$, which is consistent with higher level CASSCF/CI and MRCI+Q calculations.[37−39] The Fe−H stretching frequency is predicted as 1785 $cm^{-1}$ (B3LYP), which is just above the gas-phase value of 1758.7 $cm^{-1}$. We note that the frequency of FeH is overestimated by 100 $cm^{-1}$ with the MCPF calculation and underestimated by 90 $cm^{-1}$ with MRCI+Q. Similarly the RuH molecule is calculated to have a $^4\Sigma$ ground state, and the harmonic frequency is 1981 $cm^{-1}$ (B3LYP). For comparison the doublet state of RuH is higher in energy. Finally, OsH is predicted to have a $^4\Sigma$ ground state and 2197 $cm^{-1}$ harmonic vibrational frequency. Clearly, the fundamental frequency of the group 8 monohydride molecules increases going down the family.

The geometry and vibrational frequencies of $FeH_2$ have been calculated with several quantum chemical methods. Our B3LYP calculations gave a quasi-linear structure with 161.8° H−Fe−H bond angle and quintet ground state (Table 4); however, the BPW91 functional calculation gave higher harmonic stretching frequencies of 1761 $cm^{-1}$ ($a_1$, 39) and 1712 $cm^{-1}$ ($b_2$, 373 km/mol), which is not the usual relationship between these calculations.[40] DFT is only approximate here without attending to spin−orbit and Renner−Teller coupling, which is accounted for in a recent theoretical investigation.[39] Nevertheless, our harmonic calculation (B3LYP) predicts the strong antisymmetric mode at 1698 $cm^{-1}$, which is about 2.2% high and the more difficult to determine bending mode at 267 $cm^{-1}$, which is 20% too low. The $^3B_1$ state for $FeH_2$ is 11 kcal/mol higher in energy, and interestingly it has a 102.7° valence angle and substantially higher frequencies. The bent $^1A_1$ state is 58 kcal/mol higher in energy with still higher frequencies (Table 4), which will be important in the discussion that follows.

With the same calculation $RuH_2$ is predicted to have a $^3B_1$ ground state and H−Ru−H bond angle of 98.3° (Table 5). The

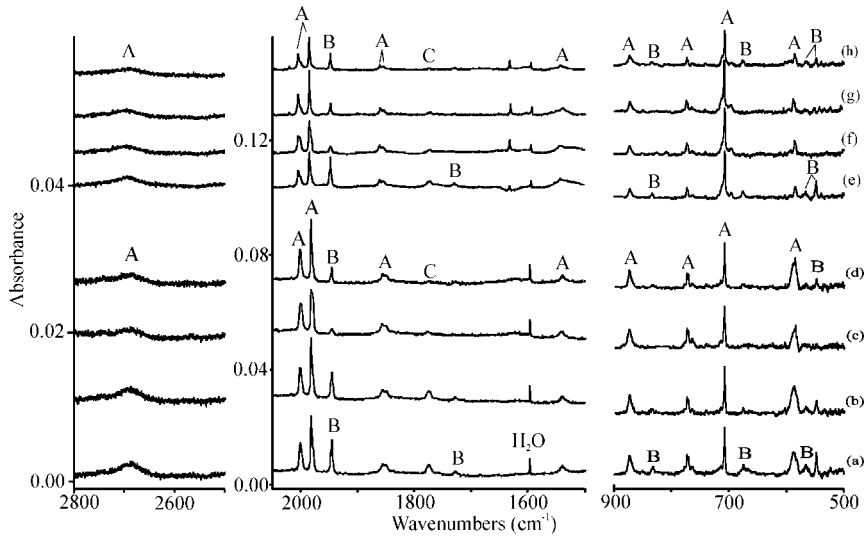


**Figure 4.** Infrared spectra for the ruthenium atom and $H_2$ reaction products in pure $H_2$ at 4.5 K: (a) Ru + $H_2$ deposition for 30 min, (b) after >380 nm irradiation, (c) after >220 nm irradiation, (d) after annealing to 6.5 K, (e) Ru + *p*-$H_2$ deposition for 30 min, (f) after >220 nm irradiation, (g) after annealing to 6.0 K, (h) after annealing to 6.5 K.

singlet and quintet states of $RuH_2$ are higher in energy. This large ground state geometry change from $FeH_2$ to $RuH_2$ indicates different hybrid prototypes: $FeH_2$ with sp hybrid prefers high-spin in d orbitals but $RuH_2$ favors sd hybridization. Higher level CASSCF calculations locate the same bent ground state for ruthenium dihydride.[41] Our calculations for $OsH_2$ also find a bent triplet ground state with H−Os−H bond angle of 105.5° (Table 6) that is very similar to $RuH_2$.

When one $H_2$ moiety is associated with $FeH_2$ on the quintet surface, there is no binding, and although the bis-dihydrogen complex $(H_2)Fe(H_2)$ ($^3B_1$, $D_{2d}$) is converged as the most stable $FeH_4$ stoichiometry structure on the triplet surface, it is 20 kcal/mol higher energy than $FeH_2$ and $H_2$. However, with three and four $H_2$ molecules available stable $FeH_2(H_2)_{2,3}$ supercomplexes are obtained, and on the singlet surface stable complexes are obtained with 2, 3, and 4 ligands. These higher complexes are also characterized by bent $FeH_2$ subunits and higher $FeH_2$ stretching and bending frequencies (Table 4). We employ the B3LYP density functional to predict binding energies in these simple dihydrogen compexes, as a model for such complexes prepared in solid hydrogen. Unfortunately,we are not able to account for the second solvation shell of $H_2$ molecules in the surrounding matrix cage, and we do not know how these interactions will affect the relative stability of singlet and triplet supercomplexes. With this in mind, consider the following reactions and energetics.

$$FeH_2(^5A_1) + 3H_2 \rightarrow FeH_2(H_2)_3(^3A) \qquad \Delta E = -9 \text{ kcal/mol} \quad (1)$$

$$FeH_2(^5A_1) + 3H_2 \rightarrow FeH_2(H_2)_3(^1A) \qquad \Delta E = +1 \text{ kcal/mol} \quad (2)$$

$$FeH_2(^5A_1) + 4H_2 \rightarrow FeH_2(H_2)_4(^1A) \qquad \Delta E = -14 \text{ kcal/mol} \quad (3)$$

The low-spin tetrahydride $FeH_4$ in the $^1A_1$ state is found on the singlet surface to be 29 kcal/mol higher in energy than the triplet bis-dihydrogen complex, so this is a stable but very high energy molecule. In addition, when three, four, and five $H_2$ molecules interact with Fe on the singlet surface, binary $FeH_2(H_2)_{2,3}$ complexes are converged with real frequencies, but these are 25 and 10 kcal/mol higher in energy, respectively, than their triplet counterparts: however, the singlet $FeH_2(H_2)_4$ complex is 14 kcal/mol lower in energy than $FeH_2$ and four $H_2$ molecules. All of these would probably be more stable if the second solvation shell of dihydrogen molcules in the solid could be included in the calculation.

In contrast $RuH_4$ and $OsH_4$ with tetrahedral structures and singlet states are predicated to be global energy minima. Figure 10 shows the energy profile as Ru is successively associated with five $H_2$ molecules to give the ultimate formation of the $RuH_2(H_2)_4$ supercomplex. Attempts to converge a higher complex with five dihydrogen ligands gave dissociation back to $RuH_2(H_2)_4$, which is then the highest ruthenium dihydride complex that can be formed. The analogous Os complex $OsH_2(H_2)_4$ was also calculated to be even more stable, which is listed in Table 6. The average $H_2$ ligand binding energy to $+RuH_2$ is 15 kcal/mol and to $OsH_2$ is 24 kcal/mol in these complexes.

The iron trihydride has been calculated with the CCSD(T) method, and pyramidal $FeH_3$ ($C_{3v}$) with high-spin $^6A'$ state was reported as the stable ground state structure.[13] In our DFT calculation the coplanar $(H_2)FeH$ complex with $^4B_2$ ground state is predicted to be the global minimum energy species. The H−H distance 0.814 Å calculated at the B3LYP level of theory is longer than H−H (0.765 Å) in $(H_2)CrH$ and free H−H (0.749 Å),[25] indicating a strong interaction between FeH and $H_2$, but the H−H bond is still retained. Optimization on the doublet electronic surface leads to a pyramidal structure 20 kcal/mol higher in energy. Similar calculations have been done for ruthenium and osmium trihydride, and the lower energy $(H_2)MH$ complex structure is converged in both doublet and quartet electronic states, which is in accord with our finding for $(H_2)FeH$.

## Discussion

New infrared absorptions will be assigned to group 8 metal hydrides and their dihydrogen complexes in solid hydrogen and neon based on $D_2$, $H_2 + D_2$, and HD substitution and agreement with DFT frequency calculations.

**$FeH_2$.** Infrared spectra of $FeH_2$ have been reported in solid Ar, Kr, and Xe matrixes and in the gas phase.[8−11] The absorption

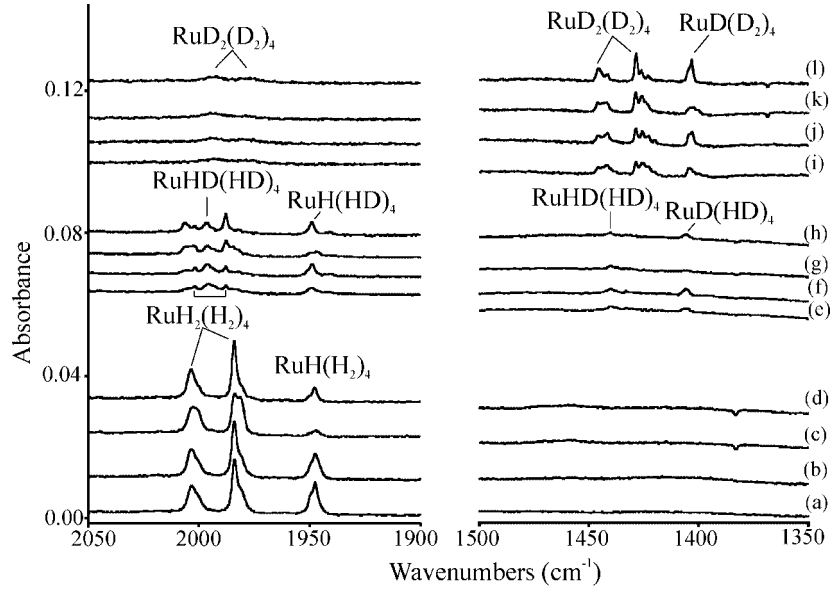


**Figure 5.** Infrared spectra for the ruthenium atom and $H_2$ reaction products in pure $H_2$ at 4.5 K: (a) Ru + $H_2$ deposition for 30 min, (b) after >380 nm irradiation, (c) after >220 nm irradiation, (d) after annealing to 6.5 K, (e) Ru + HD deposition for 30 min, (f) after annealing to 7 K, (g) after 240−380 nm irradiation, (h) after annealing to 8.5 K, (i) Ru + $D_2$ deposition for 30 min, (j) after annealing to 8 K, (k) after 240−380 nm irradiation, (l) after annealing to 10 K.

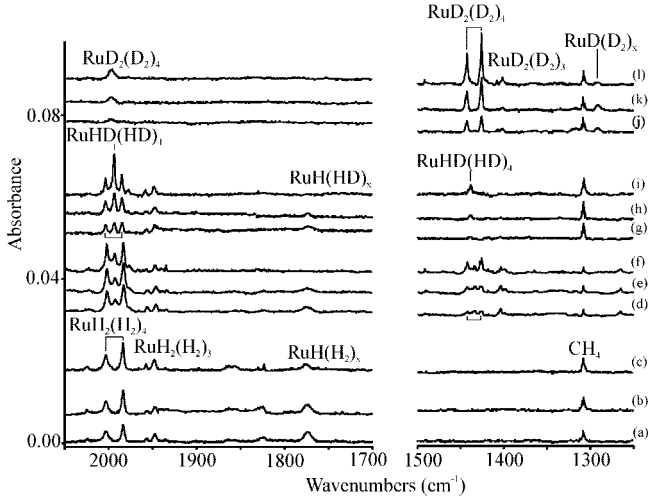


**Figure 6.** Infrared spectra for the ruthenium atom and $H_2$ reaction products in neon at 4.5 K: (a) Ru + $H_2$ (2%) deposition for 60 min, (b) after >290 nm irradiation, (c) after annealing to 10 K, (d) Ru + $H_2$ (2%) + $D_2$ (2%) deposition, (e) after >290 nm irradiation, (f) after annealing to 10 K, (g) Ru + HD (4%) deposition, (h) after >290 nm irradiation, (i) after annealing to 12 K, (j) Ru + $D_2$ (4%) deposition, (k) after >290 nm irradiation, (l) after annealing to 12 K.

of $FeH_2$ in present neon matrix at 1674.6 $cm^{-1}$ is essentially the same as the recent gas value. With $D_2$ in neon this band shifts to 1210.0 $cm^{-1}$, giving 1.3840 H/D isotopic ratio. In a pure hydrogen matrix a very sharp and strong band at 1666.4 $cm^{-1}$ is due to the same $FeH_2$ molecule, which was observed on deposition, decreased on annealing to 6 K and further reduced on >290 nm photolysis, but partly restored on >220 nm broadband irradiation. The frequency of $FeH_2$ in solid hydrogen is sufficiently close to the solid neon and gas phase values to suggest that the ground state $FeH_2$ molecule does not interact significantly with the surrounding hydrogen matrix cage any more than it does with neon. The absorption of $FeD_2$ in a pure $D_2$ matrix appeared at 1205.7 $cm^{-1}$ showing the same behavior (H/D ratio 1.3821). With neat HD two new bands at 1693.5 $cm^{-1}$ in Fe−H stretching region and 1218.3 $cm^{-1}$ in Fe−D stretching region were observed, which are due to Fe−H/Fe−D stretching modes of FeHD. In addition two bands at 1665.1 and 1207.7 $cm^{-1}$ must be the absorptions of $FeH_2$ and $FeD_2$, which show slight shifts from $FeH_2$ in pure $H_2$ and $FeD_2$ in $D_2$ because of different matrix interactions. Since there is no additional absorption tracking with the strong antisymmetric Fe−H stretching mode of $FeH_2$ in solid hydrogen, assignment to a complex like the Ru case below can be ruled out.

**$(H_2)_xFeH$.** A new band at 1713.6 $cm^{-1}$ with lower components at 1704.7 and 1698.5 $cm^{-1}$ in the pure hydrogen matrix observed on deposition increases slightly on annealing to 6 K and on near UV photolysis, but decreases on broadband irradiation and further annealing. In pure $D_2$ these bands shift to 1235.6, 1228.1 and 1222.3 $cm^{-1}$, respectively. In pure HD two groups of bands in Fe−H stretching region (1715.8, 1706.7, 1698.8 $cm^{-1}$) and Fe−D stretching region (1235.7, 1229.8, 1223.6 $cm^{-1}$) were observed, suggesting Fe−H or Fe−D stretching vibrations perturbed slightly by HD ligands. The molecular complexes, $(H_2)_xFeH$, are proposed. These bands are located slightly lower than the absorption for diatomic FeH in the gas phase (1758.7 $m^{-1}$) and the argon matrix assignment to isolated FeH (1766.4 $cm^{-1}$).[7,10] In solid neon a similar band at 1728.7 $cm^{-1}$ is found for $(H_2)_xFeH$ and 1228.6 $cm^{-1}$ band for $(D_2)_xFeD$ where, in the more slowly condensing solid neon matrix, FeH could not be isolated from the reagent $H_2$ molecule. In the case of FeH, weak complexes with $H_2$ apparently do not alter the ground electronic state of the core FeH molecule.

DFT calculations substantiate the assignment of $(H_2)_xFeH$ complexes using $x = 1$ as a model. First, with the B3LYP functional the Fe−H stretching mode in $(H_2)FeH$ is computed at 1759.0 $cm^{-1}$, only overestimated by 30 $cm^{-1}$ compared to the neon observation (1728.7 $cm^{-1}$), which is compatible with calculated and observed frequencies for other iron hydrides. For example the Fe−H stretching mode is overestimated by 24 $cm^{-1}$ for $FeH_2$. Second, the calculated Fe−H vibration in $(H_2)FeH$ (B3LYP) is 26 $cm^{-1}$ lower than this mode in diatomic FeH, which matches the frequency difference between 1728.7 $cm^{-1}$ for $(H_2)FeH$ and 1758.7 $cm^{-1}$ for the FeH (gas phase value).[7] Although we did not observe the absorption for FeH in solid

**TABLE 2: Infrared Absorptions ($cm^{-1}$) Observed from Reaction of Ruthenium and Dihydrogen in Neon, and Pure Hydrogen and Their Assignments**

| neon | | | hydrogen | | | |
|---|---|---|---|---|---|---|
| $H_2$ | HD | $D_2$ | $H_2$ [*p*-$H_2$] | HD | $D_2$ | ident |
| | | | 2690 [2692] | | | $RuH_2(H_2)_4$ |
| | | 1997 | | | 1994, 1978 | $RuD_2(D_2)_4$ |
| 2003.5 | 2003.5 | | 2003.3 [2004.8] | 2006.7 | | $RuH_2(H_2)_4$ |
| | 1994.1 | | | 1996.9 | | $RuHD(HD)_4$ |
| 1983.9 | 1985.2 | | 1983.9 [1985.2] | 1988.2 | | $RuH_2(H_2)_4$ |
| | | 1442.5 | | | 1445.2 | $RuD_2(D_2)_4$ |
| | 1438.6 | | | 1436.9 | | $RuHD(HD)_4$ |
| | | 1425.6 | | | 1428.3 | $RuD_2(D_2)_4$ |
| 1957.6 | 1958.8 | | | | | $RuH(H_2)_4$ site |
| 1947.6 | 1948.5 | | 1947.5 [1947.7] | 1949.0 | | $RuH(H_2)_4$ |
| | | 1407.8 | | | | $RuD(D_2)_4$ site |
| | 1404.2 | 1401.2 | | 1405.9 | 1403.1 | $RuD(D_2)_4$ |
| 1857.6 | | | 1857.1 [1861.0] | | | $RuH_2(H_2)_4$ |
| 1851.8 | | | 1850.1 [1855.3] | | | $RuH_2(H_2)_4$ |
| | 1342.1 | 1341.9 | | | 1337.9 | $RuD_2(D_2)_4$ |
| | 1334.9 | 1334.2 | | | 1330.8 | $RuD_2(D_2)_4$ |
| 1774.5 | 1773.6 | | 1775.7 [1775.2] | 1771.7 | | $RuH(H_2)_x$ |
| | | 1292.3 | | | 1292 | $RuD(D_2)_x$ |
| | | | 1729.5 [1729.5] | | | $RuH(H_2)_4$ |
| 1543.8 | 1546.3 | | 1540.6 [1542.7] | | | $RuH_2(H_2)_4$ |
| | | 1125.7 | | | | $RuD_2(D_2)_4$ |
| 873.1 | | | 873.9 [872.7] | | | $RuH_2(H_2)_4$ |
| | | | 833.1 [833.4] | | | $RuH(H_2)_4$ |
| | | 652.3 | | | 652.2 | $RuD_2(D_2)_4$ |
| 776.2 | | | 773.8 [773.5] | | | $RuH_2(H_2)_4$ |
| 773.1 | | | 771.8 [770.9] | | | $RuH_2(H_2)_4$ |
| 709.8 | | | 708.5 [707.3] | | | $RuH_2(H_2)_4$ |
| | | | 675.6 [675.2] | | | $RuH(H_2)_4$ |
| | | 556.3 | | | 555.6 | $RuD_2(D_2)_4$ |
| | | | 588.2 [586.3] | | | $RuH_2(H_2)_4$ |
| | | | 567.6 [567.0] | | | $RuH(H_2)_4$ |
| | | | 549.0 [548.6] | | | $RuH(H_2)_4$ |

**TABLE 3: Infrared Absorptions ($cm^{-1}$) Observed from Reaction of Osmium and Dihydrogen in Argon, Pure Hydrogen, and Neon**

| argon | | | hydrogen | | | neon | | | |
|---|---|---|---|---|---|---|---|---|---|
| $H_2$ | HD | $D_2$ | $H_2$ | HD | $D_2$ | $H_2$ | HD | $D_2$ | ident |
| 1994.9 | | | | | | | | | $OsH(H_2)_x$ |
| | | 1437.2 | | | | | | | $OsD(D_2)_x$ |
| 1935.1 | | | 1993.8 | 1993.8 | | 1992.2 | 1992.2 | | $OsH(H_2)_x$ |
| | | 1399.2 | | 1433.1 | 1431.2 | | 1433.5 | 1434.0 | $OsD(D_2)_x$ |
| | | | 1962.1 | | 1421.1 | 1957.4 | | 1416.7 | $Os_xH_y$ |
| 1873.6 | | | 1930.6 | 1930.4 | | 1932.2 | 1930.8 | | $OsH(H_2)_x$ |
| | | 1346.4 | | | 1391.0 | | | 1390.7 | $OsD(D_2)_x$ |

neon and hydrogen, the argon matrix observation at 1766.4 $cm^{-1}$ predicts the absorption for FeH in the 1770−1750 $cm^{-1}$ region.

There is no evidence for absorptions due to iron trihydride, $FeH_3$, in this experiment. The $FeH_3$ molecule is not expected to form or to survive in the low temperature matrix because of higher energy relative to the $(H_2)FeH$ complex (Table 4). Furthermore no experimental absorptions match the calculated frequencies for either $^2A_1$ or $^6A_1$ states of $FeH_3$.[13] Thus, the 1646 $cm^{-1}$ absorption assigned previously[10] to the trihydride must be due to something else, possibly a diiron species.

**$FeH_2(H_2)_3$.** In the reactions of atomic Fe with $H_2$ in pure $H_2$, two higher frequency bands at 1830.4 and 1913.5 $cm^{-1}$ track together and with lower 1088, 1056, and 633.0 $cm^{-1}$ bands. These absorptions appeared on deposition, increased slightly on annealing to 6 K, and formed a reversible photochemical equilibrium with isolated $FeH_2$ on >290 and >220 nm irradiation cycles (Figure 2). In pure $D_2$ the counterparts are found at 473.2, 1331.5, and 1389.8 $cm^{-1}$, and give 1.338, 1.375, and 1.377 H/D isotopic frequency ratios, respectively. Accordingly, the new 1830.4 and 1913.5 $cm^{-1}$ absorptions are due to Fe−H stretching vibrations while the 633.0 $cm^{-1}$ band involves a $FeH_2$ bending mode in a new species that appears to include a bent $FeH_2$ moiety. However, these modes are much higher than the corresponding vibrational motions for isolated quasi-linear $FeH_2$ described above, but they are very near the 1930 and 1865 $cm^{-1}$ values for the organometallic $FeH_2(H_2)L_3$ complex.[14] Furthermore, M−$(H_2)$ stretching modes have been observed in the 900−1500 $cm^{-1}$ region,[42] and the 1088, 1056 $cm^{-1}$ bands invite consideration of dihydrogen ligands side bound to the $FeH_2$ subunit. We looked carefully but unsuccessfully for a broad H−H stretching mode in the 2000 $cm^{-1}$ region; however, a weak, sharp, associated 2420 $cm^{-1}$ band is probably due to the combination mode of 633 and 1830 $cm^{-1}$ fundamentals. Thus, we assign this group of bands to a $FeH_2(H_2)_x$ complex, and the problem now is to determine the electronic state and the value of *x*. The large blue shift in the Fe−H stretching modes from the quintet $FeH_2$ value indicates that the $FeH_2$ core in this dihydrogen complex has a different electronic multiplicity. In

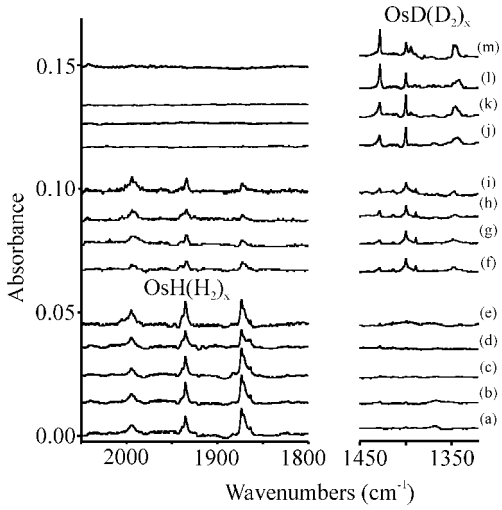


**Figure 7.** Infrared spectra for the osmium atom and $H_2$ reaction products in argon at 4.5 K: (a) Os + $H_2$ (5%) deposition for 60 min, (b) after annealing to 18 K, (c) after >380 nm irradiation, (d) after >220 nm irradiation, (e) after annealing to 30 K, (f) Os + HD (5%) deposition for 60 min, (g) after annealing to 18 K, (h) after >220 nm irradiation, (i) after annealing to 30 K, (j) Os + $D_2$ (5%) deposition for 60 min, (k) after annealing to 18 K, (l) after >220 nm irradiation, (m) after annealing to 25 K.

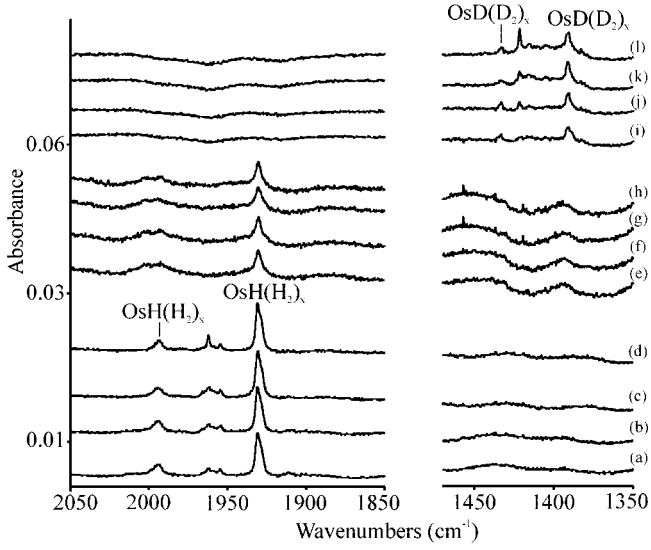


**Figure 8.** Infrared spectra for the osmium atom and $H_2$ reaction products in pure $H_2$ at 4.5 K: (a) Os + $H_2$ deposition for 30 min, (b) after >380 nm irradiation, (c) after 240−380 nm irradiation, (d) after annealing to 6.2 K, (e) Os + HD deposition for 30 min, (f) after annealing to 8 K, (g) after 240−380 nm irradiation, (h) after annealing to 9 K, (i) Os + $D_2$ deposition for 30 min, (j) after annealing to 8 K, (k) after 240−380 nm irradiation, (l) after annealing to 9 K.

addition, the strongest absorptions of this species were observed at 627.1, 1839.3, and 1921.2 $cm^{-1}$ in solid neon, which shift to 472.8, 1335.9, and 1394.3 $cm^{-1}$ in the Fe + $D_2$ reaction. With HD in neon bands at 1839.2 and 518.7 $cm^{-1}$ were observed, which is similar to the isotopic pattern found in solid HD.

With pure HD only one band at 1834.4 $cm^{-1}$ was observed in the upper Fe−H stretching region, which suggests that the two Fe−H bonds are not equivalent, a property common with the $FeH_2(H_2)L_3$ complex.[14] We note that essentially the same 1834.1 $cm^{-1}$ band and 533.0, 519.6 $cm^{-1}$ split bending mode appeared with $H_2$ + $D_2$, indicating that H, D exchange occurs within this complex, as found for the present ruthenium product and other similar complexes.[27a,43] We find the zero point energy

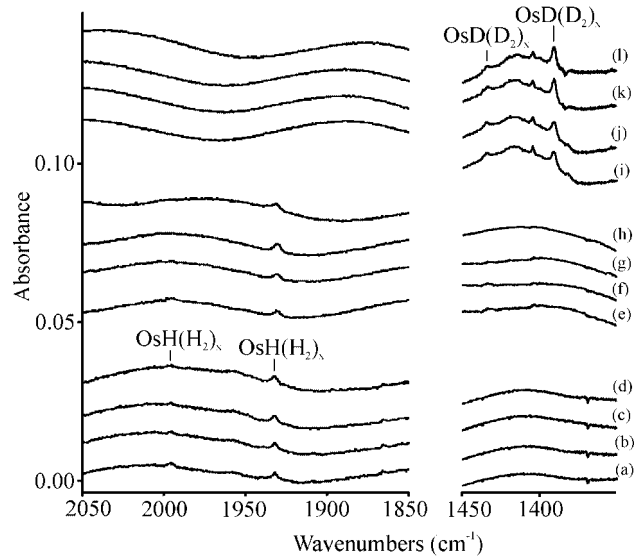


**Figure 9.** Infrared spectra for the osmium atom and $H_2$ reaction products in neon at 4.5 K: (a) Os + $H_2$ (4%) deposition for 60 min, (b) after annealing to 8 K, (c) after 240−380 nm irradiation, (d) after annealing to 10 K, (e) Os + HD (4%) deposition for 60 min, (f) after annealing to 8 K, (g) after 240−380 nm irradiation, (h) after annealing to 12 K, (i) Os + $D_2$ (4%) deposition for 60 min, (j) after annealing to 9 K, (k) after 240−380 nm irradiation, (l) after annealing to 12 K.

about 0.1 kcal/mol lower for the $FeHD(HD)_3$ complex with H in the longer bond and D in the shorter bond position to iron. This is consistent with our observation of the longer Fe−H bond (trans to HD ligand, 1834.4 $cm^{-1}$) stretching mode and not the shorter Fe−H bond (trans to vacancy, expected but not observed near 1915 $cm^{-1}$). The corresponding shorter Fe−D bond stretching mode with lower intensity expected near 1390 $cm^{-1}$ for the complex formed was not observed, but even with the all-D species this band is only 20% of the intensity of the longer Fe−D bond stretching mode. The present assignment requires H and D isotopic positional selectivity for the lower zero point energy structural isomer. In the lower region the 633.0 $cm^{-1}$ $FeH_2$ bending mode shifts to 473.2 $cm^{-1}$ for $FeD_2$ with two bands slightly below the median at 534.9 and 519.6 $cm^{-1}$ for HFeD bending split from coupling to HD ligands.

We favor assignment to the singlet $FeH_2(H_2)_3$ complex because it is the only one found with nonequivalent Fe−H bonds, and the computed Fe−H stretching frequency separation, 85 $cm^{-1}$, is nearly the same as observed, 83 $cm^{-1}$. In addition, the calculated mostly longer (1830.4 $cm^{-1}$) and shorter (1912.5 $cm^{-1}$) Fe−H bond stretching modes are 4.7 and 4.6% higher than observed, which is as expected for B3LYP,[40] the calculated Fe−($H_2$) modes are very close, and the calculated $FeH_2$ bending frequency is near the observed 633 $cm^{-1}$ value. Although this complex probably has weaker interactions with additional $H_2$ molecules present in the pure hydrogen and neon matrices, we cannot calculate these second-shell interactions. We note that the higher $FeH_2(H_2)_4$ complex is computed to be even more stable, reaction (3), but this higher complex is ruled out because the two hydrides are equivalent and separated by only 30 $cm^{-1}$ whereas the complex we observe has nonequivalent hydrides and more widely separated frequencies. The structure of the singlet $FeH_2(H_2)_3$ complex is illustrated in Figure 11. The favored $FeHD(HD)_3$ species has H in the longer hydride bond trans to the HD ligand.

Some comparisons with the Kubas iron complex $FeH_2(H_2)(L)_3$ (L = $PEtPh_2$)[14] are striking. First the Fe−H stretching modes for the Kubas complex in fluorolube at 1930 and 1865 $cm^{-1}$

**TABLE 4: Calculated Structures and Vibrational Frequencies ($cm^{-1}$) for Iron Hydrides[a]**

| species | state | structure, Å, deg | rel energy (kcal/mol) | frequencies, $cm^{-1}$ (symmetry, intensities, km/mol) |
|---|---|---|---|---|
| FeH | $^4\Delta$ | FeH: 1.573 | 0 | FeH: 1785.3(81); FeD: 1274.0(41) |
| FeH | $^4\Sigma$ | FeH: 1.623 | 33 | FeH: 1665.4(142); FeD: 1188.4(72) |
| $FeH_2$ | $^5A_1$ | FeH: 1.645<br>HFeH: 161.8 | 0 | $FeH_2$: 1773.6($a_1$,7), 1698.0($b_2$,796), 266.9($a_1$,266)<br>$FeD_2$: 1255.5(4), 1221.3(412), 191.9(138) |
| $FeH_2$ | $^3B_1$ | FeH: 1.533<br>HFeH: 102.7 | 11 | $FeH_2$: 1823.1($a_1$,35), 1792.7($b_2$,223), 660.1($a_1$,100)<br>$FeD_2$: 1299.7(19), 1281.6(116), 471.3(51) |
| $FeH_2$ | $^1A_1$ | FeH: 1.498<br>HFeH: 105.8 | 58 | $FeH_2$: 2064($a_1$,67), 1906($b_2$,66), 854($a_1$,77)<br>$FeD_2$: 1299.7(19), 1281.6(116), 471.3(51) |
| $FeH_2^-$ | $^4\Delta_g$ | FeH: 1.670<br>HFeH: 180.0 | | $FeH_2^-$: 1554($\sigma_g$,0), 1412($\sigma_u$,665), 530, 396($\pi_u$,530,83) |
| $(H_2)FeH$ ($C_{2v}$) | $^4B_2$ | FeH: 1.601<br>FeH′: 1.749<br>H′H′: 0.814 | 0 | $(H_2)FeH$: 3274.0($a_1$,321), 1759.0($a_1$,121), 1380.3($b_2$,0), 884.2($a_1$,25), 439.8($b_2$,118), 325.7($b_1$,122)<br>$(D_2)FeD$: 2316.6(161), 1253.5(59), 978.8(0), 636.4(13), 317.2(60), 235.5(62) |
| $(H_2)FeH$ ($C_{2v}$) | $^4A_2$ | FeH: 1.597<br>FeH′: 1.701<br>H′H′: 0.826 | 3 | $(H_2)FeH$: 3127.9($a_1$,377), 1755.2($a_1$,163), 1458.9($b_2$,3), 977.6($a_1$,21), 445.4($b_2$,141), 229.6($b_1$,413) |
| $FeH_3$ ($C_{3v}$) | $^6A_1$ | FeH: 1.626<br>HFeH: 117.6 | 27 | $FeH_3$: 1746($a_1$,8), 1720(e,128×2), 623(e,36×2), 358($a_1$,242) |
| $FeH_3$ ($C_{3v}$) | $^2A_1$ | FeH: 1.503<br>HFeH: 102.7 | 32 | $FeH_3$: 1927($a_1$,10), 1925(e,171 × 2), 724($a_1$,86), 630(e,17 × 2) |
| $Fe(H_2)_2$ ($D_{2d}$) | $^3B_1$ | FeH: 1.616<br>HH: 0.907 | 0 | $Fe(H_2)_2$: 2345($b_2$,1354), 2261($a_1$,0), 1718(e,51×2), 1186($a_1$,0), 1080($b_1$,0), 933($b_2$,897), 309(e,25×2) |
| $FeH_4$ | $^1A_1$ | FeH: 1.492<br>HFeH: 109.5 | 29 | $FeH_4$: 2038($a_1$,0), 2020($t_2$,423), 837(e,0), 820($t_2$,159) |
| $FeH_2(H_2)_3$ | $^1A$ | FeH: 1.479, 1.530<br>HFeH: 88.1<br>FeH′: 1.660, 1.710, 1.960<br>H′H′: 0.768, 0.834 | 10 | $FeH_2(H_2)_3$: 3061 (53), 3058(189), 2936 (276), 2001 (41), 1916 (212), 1861 (2), 1819 (41), 1793 (21), 1183 (1), 1075 (92), 1053 (71), 817 (16), 757 (0), 746 (28), 686 (13), 637 (66), 594 (53), 547 (105), 469 (2), 460 (0), 380 (2). The strongest $FeH_2(H_2)_4$ modes are 3148 (160), 1982 (130), 1952 (155), 1084 (54), 1057 (68), 630 (122) |
| $FeH_2(H_2)_3$ | $^3A$ | FeH: 1.539<br>HFeH: 77.6<br>FeH′: 1.660, 1.710, 1.960<br>H′H′: 0.768, 0.834 | 0 | $FeH_2(H_2)_3$: 3983 (26), 3082(274), 3045 (99), 1889 (96), 1852 (143), 1651 (51), 1639 (1), 1007 (11), 989 (45), 904 (4), 776 (0), 686 (40), 620 (9), 606 (7), 578 (16), 568 (3), 476 (91), 385 (4), 381 (2), 321 (16), 160 (1). The strongest $FeH_2(H_2)_2$ modes are 3070 (305), 1897 (92), 1855 (162), 985 (48), 723 (40), 478 (106) |

[a] Calculations used B3LYP/6-311++G(3df,3pd).

**TABLE 5: Calculated Structural Parameters and Vibrational Frequencies ($cm^{-1}$) for Ruthenium Hydrides[a]**

| species | state | structure, Å, deg | rel energy (kcal/mol) | frequencies, $cm^{-1}$ (symmetry, intensities km/mol) |
|---|---|---|---|---|
| RuH | $^4\Sigma$ | RuH: 1.620 | 0 | RuH: 1980.8(166); RuD: 1407.9(84) |
| RuH | $^2X$ | RuH: 1.598 | 32 | RuH: 2020.8(170); RuD: 1436.5(86) |
| $RuH_2$ | $^3B_1$ | RuH: 1.581<br>HRuH: 98.3 | 0 | $RuH_2$: 2082.3($a_1$,56), 2023.4($b_2$,210), 715.2($a_1$,62)<br>$RuD_2$: 1479.2(28), 1439.3(107), 508.7(31) |
| $RuH_2$ | $^5A_1$ | RuH: 1.697<br>HRuH: 141.8 | 17 | $RuH_2$: 1814($a_1$,65), 1711($b_2$,269), 728($a_1$,53) |
| $RuH_2$ | $^1A_1$ | RuH: 1.558<br>HRuH: 90.3 | 21 | $RuH_2$: 2163($a_1$,59), 2095($b_2$,215), 694($a_1$,39) |
| $(H_2)RuH$ ($C_s$) | $^4A''$ | RuH: 1.639<br>RuH′: 1.887<br>H′H′: 0.806<br>HRuH′: 167.5 | 0 | $(H_2)RuH$: 3426.3(a′,215), 1886.1(a′,310), 1326.0(a″,3), 779.6(a′,14), 580.9(a″,15), 578.2(a′,16)<br>$(D_2)RuD$: 2424.0(108), 1339.3(155), 939.9(1), 557.1(8), 415.9(7), 413.1(8) |
| $RuH(H_2)_4$ | $^2A$ | RuH: 1.611<br>RuH′: 1.723−1.823<br>H′H′: 0.831−0.874 | | $RuH(H_2)_4$: 3116(189), 3085(91), 2826(151), 2706(122), 2015(146), 1824(10), 1791(28), 1565(19), 1419(7), 1208(25), 946(36), 921(150), 830(8), 820(4), 708(42),661(25), 605(38), 581(17), 571(50), 563(33), 496(3), 393(2), 358(0), 301(1) |
| $RuH_4$ ($T_d$) | $^1A_1$ | RuH: 1.567 | | $RuH_4$: 2169.4($a_1$,0), 2146.6($t_2$,107×3), 929.3(e,0×2), 759.6($t_2$,80×3)<br>$RuD_4$: 1534.6(0), 1528.8(56×3), 657.3(0×2), 543.7(41×3) |
| $RuH_2(H_2)_4$ | $^1A$ | RuH: 1.602<br>HRuH: 81.2<br>RuH′: 1.692...<br>H′H′: 0.833, 0.876 | | $RuH_2(H_2)_4$: 3123.2(97), 3111.9(102), 2749.3(155), 2700.4(1), 2084.3(107), 2045.1(138), 1929.7(28), 1923.5(42), 1605.6(54), 1600.7(9), 1299.5(0), 979.2(2), 960.9(119), 909.1(31), 869.8(4), 826.2(32), 819.9(43), 733.0(103), 667.3(32), 625.2(25), 624.1(39), 601.3(17), 584.0(52), 500.2(13), 453.6(4), 442.6(0), 352.8(1)<br>$RuD_2(D_2)_4$: 2209.9(48), 2202.2(50), 1948.5(74), 1901.2(1), 1481.3(48), 1450.6(64), 1367.1(17), 1362.6(24), 1137.5(29), 1133.6(5), 919.5(0), 698.7(3), 695.6(72), 651.9(17), 616.8(2), 587.7(39), 582.1(4), 530.4(54),... |

[a] Calculations used B3LYP/6-311++G(3df,3pd)/SDD.

**TABLE 6: Calculated Structures and Vibrational Frequencies ($cm^{-1}$) for Osmium Hydrides[a]**

| species | state | structure, Å, deg | energy (kcal/mol) | frequencies, $cm^{-1}$ (symmetry, intensities, km/mol) |
|---|---|---|---|---|
| OsH | $^4\Sigma$ | OsH: 1.593 | 0 | OsH: 2196.6(46); OsD: 1557.9(23) |
| OsH | $^2X$ | OsH: 1.617 | 38 | OsH: 2123.9(54); OsD: 1506.3(29) |
| $(H_2)OsH$ | $^4A''$ | OsH:1.663<br>OsH′:1.805<br>H′H′: 0.863<br>HOsH′:166.2 | | OsH($H_2$): 2783.1(a′,270), 2018.7(a′,237), 1660.8(a″,4), 943.1(a′,9), 744.2(a′,1), 698.2(a″,3)<br>OsD($D_2$): 1969.4(136), 1430.3(118), 1176.1(2), 671.0(5), 529.9(0), 496.7(2) |
| $OsH_2$ | $^3B_1$ | OsH: 1.595<br>HOsH:105.5 | 0 | $OsH_2$: 2224.2($a_1$,23), 2209.9($b_2$,83), 659.2($a_1$,72)<br>$OsD_2$: 1576.5(12), 1568.1(42), 467.8(36) |
| | $^5A_2$ | OsH:1.688<br>HOsH:142.0 | 18 | $OsH_2$: 1962($a_1$,50), 1846($b_2$,336), 781($a_1$,17) |
| $OsH_4$ ($T_d$) | $^1A_1$ | OsH: 1.594 | 0 | $OsH_4$: 2259.2($a_1$,0), 2240.3($t_2$,63 × 3), 864.7(e,0 × 2), 786.2($t_2$,43 × 2) |
| $OsH_2(H_2)$ | $^3A_1$ | OsH:1.625<br>HOsH:65.8<br>OsH′:1.767<br>H′H: 0.943 | 29 | $OsH_2(H_2)$: 2231.9(274), 2155.8(28), 2137.7(28), 1783.7(2), 1140.4(0), 746.8(234), 458.7(37), 440.9 |
| $OsH_2(H_2)_4$ | $^1A$ | OsH:1.638<br>HOsH:81.9<br>OsH′:1.70−1.82<br>H′H: 0.94−0.86 | | $OsH_2(H_2)_4$: 2815.9(87), 2787.6(123), 2364.2(131), 2307.6(0), 2149.4(113), 2123.6(124),..., 490.7(2), 422.3(9). |

[a] Calculations used B3LYP/6-311++G(3df,3pd)/SDD.

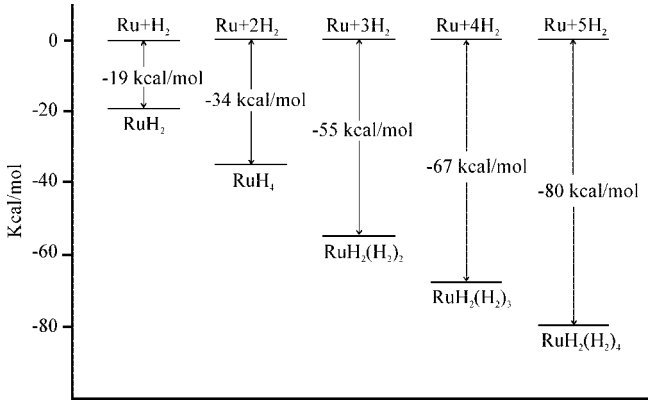


**Figure 10.** Energy profile for Ru and up to five dihydrogen molecules at the B3LYP level of theory.

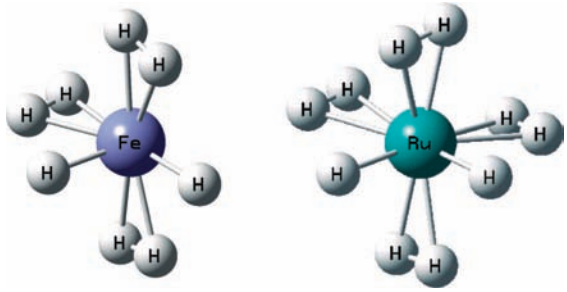


**Figure 11.** Structures calculated for singlet iron and ruthenium dihydride supercomplexes with dihydrogen at the B3LYP level of theory. The Fe−H distances are 1.479 and 1.530 Å, and the Ru−H bond lengths are both 1.602 Å.

are near our 1914 and 1830 $cm^{-1}$ absorptions in solid hydrogen. The measured Fe−H distances for the iron complex are 1.514 and 1.538 Å, and our B3LYP computed values are 1.479 and 1.530 Å. The $FeH_2$ valence angle in the organometallic complex is 88°, and our computed angle is 88°. The measured Fe−($H_2$) distances are 1.607 and 1.576 Å whereas our computed values are 1.710 and 1.660 Å. Our two most strongly bound dihydrogen ligands appear to be about as strongly bound (H−H distance 0.834 Å) as the single dihydrogen in the Kubas complex (H−H distance 0.821 Å).

Finally, we considered both charged species and diiron hydrides $Fe_2H_2$ and $Fe_2H_4$ structures as possible sources of the higher frequency 1830.4 and 1913.5 $cm^{-1}$ absorptions. The $FeH^+$ fundamental is calculated as 1873 $cm^{-1}$, and that is not high enough. The $FeH_2^-$ anion has been observed by photodetachment spectroscopy,[44] and our calculation of the strong fundamental at 1412 $cm^{-1}$ provided a basis for search, but no absorptions were found in this region. Furthermore, we performed Fe and $H_2$ experiments with $CCl_4$ added to provide a diagnostic for charged species,[29] and no effect was observed. The most stable diiron HFe(H)Fe structure has a septet ground state, and the strongest absorption at 1718 $cm^{-1}$ does not fit. Our most stable $Fe_2H_4$ structure is a quintet $C_{2h}$ with highest strong frequency calculated as 1815 $cm^{-1}$, which is not observed.

**$RuH_2(H_2)_4$.** Strong bands appeared at 2003.5 and 1983.9 $cm^{-1}$ on reaction of laser-ablated Ru with $H_2$ in solid neon, which increased slightly on annealing to 8 K, increased by 30% on >290 nm irradiation and increased slightly on further annealing to 12 K. With $D_2$ in neon these bands shift to 1442.5 and 1425.6 $cm^{-1}$, respectively, giving 1.3889 and 1.3913 H/D isotopic frequency ratios. These bands are appropriate for Ru−H stretching vibrations as found for ruthenium hydrides. With HD in neon three bands at 2003.5, 1994.1 and 1985.2 $cm^{-1}$ of equal intensity in the Ru−H stretching region and one band at 1438.6 $cm^{-1}$ in the Ru−D stretching region appeared on deposition. After annealing and irradiation the 1994.1 $cm^{-1}$ band doubled intensity while other two bands increased very little. First the new HD bands at 1994.1 and 1438.6 $cm^{-1}$ suggest the ruthenium dihydride frame (RuHD) assignment although they are not exactly median bands, and they are perturbed by HD ligands. Second, two H bands at 2003.5 and 1985.2 $cm^{-1}$ due to $RuH_2$ vibrations appeared while two D bands due to $RuD_2$ motions were absent in the HD experiment, implying the H and D atoms are exchanged between hydride and dihydrogen ligand, which favors $RuH_2(D_2)(HD)_3$ with lower zero-point energy than $RuHD(HD)_4$. Similar isotopic positional exchange in rhodium hydride dihydrogen complexes has been observed.[43] Third, on annealing the HD sample, the median bands due to RuHD subunits doubled while $RuH_2$ bands increased slightly, suggesting that the neon matrix environment limited H−D exchange

between hydride and dihydrogen ligand positions. This exchange is consistent with the fluxional nature of (classical transition metal hydride)($\eta^2$-$H_2$) complexes in general[17,18] and the thermally stable $RuH_2(H_2)(PCy_3)_3$ and $RuH_2(H_2)_2(PCy_3)_2$ complexes, which have slightly lower broad 1950 $cm^{-1}$ and 1927 and 1890 $cm^{-1}$ Ru−H stretching modes, respectively.[17c,18a]

DFT calculations performed for $RuH_2$ and its dihydrogen complexes show $RuH_2(H_2)_4$ to be the most stable complex with a maximum of four $H_2$ ligands attached to $RuH_2$.[28] The calculated frequencies of $RuH_2(H_2)_4$ include 8 strong absorptions with H−H stretching mode at 2749.3 $cm^{-1}$, Ru−H stretching modes at 2045.1 and 2084.3 $cm^{-1}$, Ru−$H_2$ stretching modes at 1923.5, 1929.7, 1606.6 $cm^{-1}$, and $RuH_2$ bending modes at 960.9 and 733.0 $cm^{-1}$. First of all the calculated Ru−H stretching modes are overestimated by only by 3% and 4%, which is appropriate for density functional theory.[40] These calculated frequencies also encouraged us to search for more absorptions in solid neon. Two weak bands at 1857.6 and 1851.8 $cm^{-1}$ and a weak band at 1543.8 $cm^{-1}$, and two strong bands at 873.1 and 709.8 $cm^{-1}$ in solid neon track with the upper Ru−H stretching modes and can be assigned to Ru−$H_2$ stretching and bending modes. The comparison between calculated and observed values shows very good agreement. With $D_2$ in solid neon the Ru−$H_2$ stretching modes shift to 1341.9, 1334.2, and 1125.7 $cm^{-1}$, respectively, giving slightly smaller H/D ratios (around 1.385) than that of W−H stretching modes. The bending modes shift to 652.3 and 556.3 $cm^{-1}$ giving only 1.338 and 1.276 H/D ratios.

Unfortunately, the H−H stretching absorption was very weak in solid neon, but the D−D counterpart was observed at 1997 $cm^{-1}$. However this mode has been identified in our pure $H_2$ experiments (Figure 4). The reaction of Ru with $H_2$ in solid hydrogen gave associated bands at 2690 $cm^{-1}$ (H−H stretching mode), 2003.3 and 1883.9 $cm^{-1}$ (Ru−H stretching modes), 1857.1, 1850.1, 1540.6, 873.9 $cm^{-1}$ (Ru−$H_2$ stretching modes), and 708.5and 588.2 $cm^{-1}$ (bending modes), which not only match neon absorptions very well but also show stronger absorbance because of more extensive reaction in the pure hydrogen matrix. The important H−H stretching modes for $RuH_2(H_2)_4$ were observed in solid hydrogen because of band enhancement. Similar experiments were also done in *p*-$H_2$, and the reaction product absorptions are essentially the same (Table 2), but the bands were slightly sharper (Figure 4). In pure $D_2$ all bands shift to the D-region at 1994 and 1978 $cm^{-1}$ (D−D stretching), 1445.2 and 1428.3 $cm^{-1}$ (Ru−D stretching), 1337.9, 1330.8 $cm^{-1}$ (Ru−$D_2$ stretching), and 652.2 and 555.6 $cm^{-1}$ (bending).

The structure[28] of $RuH_2(H_2)_4$ illustrated in Figure 11 is very similar to the structure reported recently for the slightly stronger $WH_2(H_2)_4$ complex.[27a] The palladium complex Pd($H_2$) with H−H mode at 2971 $cm^{-1}$ binds dihydrogen less strongly while the tungsten complex binds dihydrogen more strongly as the H−H stretching mode, 2500 $cm^{-1}$, is lower than the 2680 $cm^{-1}$ value observed here for $RuH_2(H_2)_4$.[27a,42]

In pure $H_2$ another band at 1947.5 $cm^{-1}$ was observed on deposition and decreased on broadband photolysis. This band shifts to 1403.8 $cm^{-1}$ upon Ru atom reaction with $D_2$ in pure deuterium. With pure HD as reagent two absorptions at 1949.0 and 1405.9 $cm^{-1}$ were found in the Ru−H and Ru-D stretching regions, respectively, near the pure $H_2$ and pure $D_2$ values, which identifies the vibration of a single Ru−H bond. Weaker bands labeled B in Figure 4 at 1729.5, 833.1, 675.6, 567.6, and 549.0 $cm^{-1}$ are associated with the stronger B band at 1947.5 $cm^{-1}$. Ultraviolet irradiation (Figure 5) decreases the B bands in favor of the A bands, and annealing reverses this process. The most likely assignment for these six B bands is to the closely related $RuH(H_2)_4$ species, which will be discussed below. We cannot suggest a simple mechanism for this process, so we believe that the above observations are independent of one another.

The present supercomplexes in solid hydrogen are a continuation of the ligated complexes[18a] $RuH_2(H_2)(PCy_3)_3$ and $RuH_2(H_2)_2(PCy_3)_2$ where our hydrogen rich environment has allowed more dihydrogen ligation to the metal center at the expense of overall complex stability as no other ligands are present in the neat hydrogen sample to compete with dihydrogen.

**RuH, $(H_2)$RuH, and $RuH(H_2)_4$.** The weak band observed at 1821.0 $cm^{-1}$ in solid argon and provisionally assigned to isolated RuH is probably identified correctly.[16] Our B3LYP calculations predict the ground state as $^4\Sigma$ with 1980.8 $cm^{-1}$ harmonic frequency (Table 5). No reasonable counterpart is observed in solid neon, and we presume that any RuH formed during laser ablation and deposition is not isolated in the softer neon matrix in the presence of excess hydrogen. Weak bands were observed at 1775 $cm^{-1}$ in reactions of Ru + $H_2$ and at 1292 $cm^{-1}$ for Ru + $D_2$ in neon, respectively, give the 1.374 H/D ratio. These bands decreased on annealing and photolysis. With HD in neon both bands appeared without shift, which suggests that only one H(D) atom is involved in the vibration, and the RuH and RuD diatomic molecules complexed to dihydrogen, $RuH(H_2)$ and $RuD(D_2)$, are appropriate for these absorptions. A weak counterpart was observed in solid hydrogen, labeled C in Figure 4.

Our calculations find a quartet $RuH(H_2)$ complex bound by 10 kcal/mol with strong Ru−H frequency about 100 $cm^{-1}$ below RuH, and higher complexes are not bound on the quartet surface. However, on the doublet surface, three higher complexes are stable. The $RuH(H_2)_2$ complex is 34 kcal/mol lower, the $RuH(H_2)_3$ complex 39 kcal/mol lower, and the highest $RuH(H_2)_4$ complex 52 kcal/mol lower in energy than $^4\Sigma$ RuH and 2, 3 or 4 $H_2$ molecules. Attempts to compute a RuH complex with five dihydrogen molecules eliminated one $H_2$ and converged again to $RuH(H_2)_4$. The six observed B frequencies correlate well with the B3LYP calculated harmonic frequencies (Table 4), which are 3−6% higher than the six observed values, except for the Ru−($H_2$) stretching mode, and our identification of doublet state $RuH(H_2)_4$ is supported by this comparison.

We note a higher yield of $RuH(H_2)_4$ relative to $RuH_2(H_2)_4$ with para-hydrogen (Figure 4). Para-hydrogen induced polarization has enabled the NMR detection of minor isomers of ruthenium dihydride organometallic complexes,[45] but the only effect we find here is generally sharper bands with slight shifts (Table 2).

**$(H_2)$OsH and $OsH(H_2)_x$.** The harmonic vibrational frequencies of diatomic OsH and OsD were calculated at 2196.6 and 1557.9 $cm^{-1}$ (H/D frequency ratio 1.410). No product absorptions are observed above 2000 and 1440 $cm^{-1}$ in solid neon, which simply means that we have not trapped these heavy diatomic molecules. The 1995.2 $cm^{-1}$ band with hydrogen in solid neon shifts to 1434.0 $cm^{-1}$ with deuterium (H/D ratio 1.3914). This is appropriate for an anharmonic Os−H vibration. With the HD reagent small shifts were observed (Table 3), and this we believe is due to the formation of complexes, $(H_2)_x$OsH and $(HD)_x$OsH, for example, which results in slight frequency shifts. Stronger bands were observed at 1932.2 and 1390.7 $cm^{-1}$ for each reagent in solid neon (H/D ratio 1.3894). These bands are appropriate for higher $x$ values in larger complexes. Unfortunately, we cannot determine $x$ nor extrapolate to $x = 0$ in these experiments.

A strong absorption at 1930.6 $cm^{-1}$ in solid hydrogen observed on deposition did not change its intensity very much on further irradiation and annealing. In solid deuterium this band shifted to 1391.0 $cm^{-1}$ giving a 1.388 H/D ratio. With pure HD only the Os−H stretching frequency at 1930.4 $cm^{-1}$ was observed suggesting strong OsH and OsD exchange in this dihydrogen−osmium hydride complex.

**Reaction Mechanisms.** Laser-ablated metal atoms react with molecular hydrogen to give primary MH (M = Fe, Ru, Os) products, which are endothermic by 13 kcal/mol (Fe) and 45 kcal/mol (Ru), and 45 kcal/mol (Os), respectively, with B3LYP functional calculations.

$$M + H_2 \rightarrow MH + H \quad (4)$$

The MH diatomic molecule is extremely reactive and further coordinates $H_2$ to give $(H_2)MH$ complexes, and these reactions are exothermic by 7 kcal/mol (Fe), 10 kcal/mol (Ru), and 14 kcal/mol (Os). The analogous $MH(H_2)(dppe)_2^+$ cation complexes are well-known in the organometallic literature.[46]

$$MH + H_2 \rightarrow (H_2)MH \quad (5)$$

The insertion reactions of bare and coordinated transition metals into the $H_2$ molecule to form metal hydrides have been investigated extensively in our group.[24−29,47,48] Most of the reactions require a large energy barrier, but some of them occur spontaneously. Our insertion reactions of Fe, Ru, and Os atoms into $H_2$ are calculated (B3LYP) to be exothermic by 40 kcal/mol (Fe), 19 kcal/mol (Ru), 25 kcal/mol (Os), respectively.

$$M + H_2 \rightarrow MH_2 \quad (6)$$

$FeH_2$ was observed in both solid neon and hydrogen matrices. However, there are no absorptions in these experiments for isolated $RuH_2$ and $OsH_2$ although these reactions are exothermic, suggesting that a larger activation energy is required for the Ru and Os insertion reactions. Apparently, insufficient $OsH_2$ was made to form stable higher complexes.

It is interesting to note that the iron tetrahydride ($FeH_4$) and dihydride complex $FeH_2(H_2)$ are not obtained in these experiments. From DFT calculations the more stable form of $FeH_4$ actually is a $Fe(H_2)_2$ complex, but this is still a higher energy species as the reaction starting with $FeH_2 + H_2$ is endothermic by 20 kcal/mol.

$$FeH_2 + H_2 \rightarrow Fe(H_2)_2 \qquad \Delta E = +20 \text{ kcal/mol} \quad (7)$$

Accordingly no further reaction was observed for $FeH_2$ with one $H_2$ molecule, and $FeH_2$ is stabilized in the pure dihydrogen matrix. In contrast the first row dihydride $CrH_2$ complexes one and two dihydrogen molecules and the stable chromium hexahydride is the $CrH_2(H_2)_2$ complex.[25] However, on the higher energy triplet and singlet potential energy surfaces, $FeH_2$ does combine with more dihydrogen molecules, as described by reactions (1) and (2) above.

The tetrahydride $RuH_4$ is 15 kcal/mol lower in energy than $RuH_2 + H_2$ and 34 kcal/mol lower than $Ru + 2H_2$ although $RuH_4$ did not appear in our experiments. It is expected that two $H_2$ molecules can coordinate to Ru, but the H−H bond is not cleaved because of high activation energy. Based on our experiments, the complex $RuH_2(H_2)_4$ is trapped in low temperature matrices, which is exothermic by 80 kcal/mol (Figure 10), suggesting that the electron configuration of atomic Ru atom is changed by the surrounding five $H_2$ molecules. This is in accord with the ruthenium carbonyl and $H_2$ reaction: only higher occupied d species, $Ru(CO)_{2-4}$, are ready to insert into $H_2$ to form hydrides $H_2Ru(CO)_{2,3,4}$ while the complex $(H_2)Ru(CO)$ is formed from the reaction of $RuCO + H_2$.[14]

$$Ru + 2H_2 \rightarrow RuH_4 \qquad \Delta E = -34 \text{ kcal/mol} \quad (8)$$

$$Ru + 5H_2 \rightarrow RuH_2(H_2)_4 \qquad \Delta E = -80 \text{ kcal/mol} \quad (9)$$

Interesting isotopic exchanges are observed in the Fe and Ru reactions with HD in solid neon and in solid HD as also found in the rhodium system.[43] In both solid HD and with HD in excess neon, $FeH_2$ and $FeD_2$ are observed (Figures 1 and 3). This implies that an energized intermediate [FeHD(HD)]* is involved in the process forming the pure isotopic species. The major product $RuHD(HD)_4$ absorptions were accompanied by $RuH_2(L)_4$ bands (where L = molecular hydrogen isotope, $H_2$, HD or $D_2$), and both increased on UV irradiation. This arises due to isotopic exchange in the initial energized complex intermediate involved reaction (9), which must begin with reaction (6). In solid HD > 220 nm irradiation decreased $RuHD(HD)_4$ absorptions and increased the $RuH_2(L)_4$ counterpart absorptions. These observations show that the dihydrogen ligands in the $RuH_2(H_2)_4$ supercomplex exchange with the hydride ligands on electronic excitation under ultraviolet irradiation. We note that $RuH_2(D_2)(HD)_3$ is about 0.1 kcal/mol lower in energy than $RuHD(HD)_4$. A like observation was found with $H_2 + D_2$ where $RuHD(L)_4$ was observed in addition to the pure isotopic hydride and deuteride species. This isotopic exchange is a manifestation of the fluxional nature of these hydride−dihydrogen complexes, which occurs at room temperature for the organometallic derivatives,[17,18] but energized conditions are required for our $RuH_2(H_2)_4$ complex to exhibit this fluxional behavior under cryogenic conditions.

Our calculations find that four $H_2$ molecules are bound more strongly to $RuH_2$ than to RuH.[28] The total binding energy is 9 kcal/mol higher, the average Ru−($H_2$) distance is 0.012 Å shorter, and the average H−H distance is 0.004 Å longer (Table 4). The unpaired electron in the doublet $RuH(H_2)_4$ complex is located on the Ru center from the computed spin density of 0.82. Structures for the product complexes illustrated in Figure 11 show very similar ligand structures.

The supercomplexes $FeH_2(H_2)_3$ and $RuH_2(H_2)_4$ have characteristics in common with the recently reported $WH_4(H_2)_4$ supercomplex.[27a] There is a definite electronic interaction between the metal centers and the dihydrogen ligands as the multiplicity of each metal dihydride is reduced in the supercomplexes, and accordingly metal valence d electrons are paired in the bonding to three or four dihydrogen ligands. In the Ru supercomplex, the average $H_2$ ligand binding energy at the B3LYP level (zpe but not bsse corrected) is 15 kcal/mol, and 15 kcal/mol was also reported for the W supercomplex.[27a] We find charge rearrangement based on computed Mulliken charges for the metal dihydrides and the supercomplexes. In the iron case, charges on the quintet $FeH_2$ molecule, +0.20 and −0.10, −0.10, change to −0.82 and −0.04, +0.07 with +0.26 on the $H_2$ ligands in the singlet trisdihydrogen complex. The singlet trisdihydrogen complex is more polar than the triplet, with charges −0.51 and −0.03, −0.03 with +0.19 on the $H_2$ ligands in the triplet trisdihydrogen complex, which may account for the trapping of the singlet instead of the triplet in the solid hydrogen matrix. In the $RuH_2$ system, the dihydride molecule charges are +0.34 and −0.17, −0.17 and these change to −0.39 and −0.05 with +0.09, 0.10, 0.11, 0.19 on the ligands. For the RuH system, the RuH molecule charges are 0.19 and −0.19, and the complex charges are −0.20, −0.08 with +0.04, 0.08, 0.09, 0.09 on the ligands. Analogous differences were found for $WH_4$ and its supercomplex.[27a] This shows that negative

charge from the dihydrogen ligands is transferred to the metal center in the bonding process. Our calculated H−H bond lengths for the Ru supercomplex are slightly shorter than those reported for the W supercomplex, and our H−H stretching frequency, 2690 $cm^{-1}$, is higher than the 2500 $cm^{-1}$ value observed for the W supercomplex. Finally, our 15 kcal/mol average $H_2$ binding energies for these metal dihydride supercomplexes are higher than the average $H_2$ binding energies recently computed for a series of metal-ethylene complexes.[49]

## Conclusions

Iron, ruthenium and osmium atoms react with $H_2$ in solid neon and pure hydrogen to give MH molecules and $MH(H_2)_x$ complexes (M = Fe, Ru, Os), the $FeH_2$ molecule, and $MH_2(H_2)_x$ complexes (M = Fe, Ru). These species are identified through isotopic substitution ($D_2$, HD, $H_2+D_2$), comparison with earlier assignments, and the DFT frequency calculations. The $FeH_2$ molecule is characterized by one strong infrared fundamental and a high spin ground state with the quasi-linear structure. Although the quintet ground state $FeH_2$ molecule is repulsive to additional $H_2$ molecules, based on computation and observation of the $FeH_2$ molecule in solid hydrogen, a stable $FeH_2(H_2)_3$ supercomplex has been identified most likely in the singlet state. This complex is weakly bound, and it may be compared to the widely investigated organometallic $FeH_2(H_2)L_3$ complexes.[14]

The isolated $RuH_2$ and $OsH_2$ molecules were not observed in our experiments because of the large activation energy required for these atomic insertion reactions with one $H_2$ molecule. However the laser ablated Ru atom reaction with 5 $H_2$ molecules produced $RuH_2(H_2)_4$, which is stabilized in solid pure $H_2$ and neon matrices. From this we conclude that the presence of extra potentially stabilizing dihydrogen ligands lowers the activation energy for the first insertion reaction. Our calculations show that this ruthenium dihydrogen complex is much more stable than the iron counterpart. The observed H−H stretching frequencies suggest that $RuH_2(H_2)_4$ is not quite as stable as the analogous tungsten complex.[27a] Our completely saturated tetradihydrogen ruthenium dihydride complex may be compared to the organometallic $RuH_2(H_2)_2L_2$ and $RuH_2(H_2)L_3$ complexes.[18a] However, no osmium dihydride complex was observed here.

The reactive MH species combine $H_2$ to form complexes $(H_2)MH$ for Fe, Ru and Os instead of trihydrides $MH_3$. The $MH_3$ species are calculated to have higher energy and M−H stretching frequencies, and these molecules are not trapped in our low temperature matrices.

**Acknowledgment.** We gratefully acknowledge financial support from NSF Grant CHE 03-52487 and NCSA computing Grant No. CHE07-0004N to L. A.

## References and Notes

(1) McLean, I. S.; Wilcox, M. K.; Becklin, E. E.; Figer, D. F.; Gilbert, A. M.; Graham, J. R.; Larkin, J. E.; Levenson, N. A.; Teplitz, H. I.; Kirkpatrick, J. D. *Astrophys. J.* **2000**, *533*, L45.

(2) (a) Tsujimoto, Y.; Tassel, C.; Hayashi, N.; Watanabe, T.; Kageyama, H.; Yoshimura, K.; Takano, M.; Ceretti, M.; Ritter, C.; Paulus, W. *Nature* **2007**, *450*, 1062. (b) Lau, C. P.; Ng, S. M.; Jia, G.; Lin, Z. *Coord. Chem. Rev.* **2007**, *251*, 2223.

(3) (a) Bullock, R. M. *Angew. Chem., Int. Ed.* **2007**, *46*, 7360. (b) Justice, A. K.; Rauchfuss, T. B.; Wilson, S. R. *Angew. Chem., Int. Ed* **2007**, *46*, 6152.

(4) Babik, S. T.; Fink, G. *J. Mol. Catal. A: Chem.* **2002**, *188*, 245.

(5) Cheng, T. Y.; Bullock, R. M *Organometallics* **2002**, *21*, 2325.

(6) Armstrong, F. A.; Fontecilla-Camps, J. C. *Science* **2008**, *321*, 498.

(7) (a) Wilson, C.; Brown, J. M. *J. Mol. Spectrosc.* **1999**, *197*, 188. (b) see alsoArmentrout, P. B.; Sunderlin, L. S. *Transition Metal Hydrides*; Dedreu, A., Ed.; VCH Publishers: New York, 1992, pp 1−64.

(8) Ozin, G. A.; McCaffrey, J. G. *J. Phys. Chem.* **1984**, *88*, 645.

(9) Rubinovitz, R. L.; Nixon, E. R. *J. Phys. Chem.* **1986**, *90*, 1940.

(10) Chertihin, G. V.; Andrews, L. *J. Phys. Chem.* **1995**, *99*, 12131.

(11) Korsgen, H.; Urban, W.; Brown, J. M. *J. Chem. Phys.* **1999**, *110*, 3861.

(12) (a) Siegbahn, P. E. M.; Blomberg, M. R. A.; Bauschlicher, C. W., Jr *J. Chem. Phys.* **1984**, *81*, 1373. (b) Granucci, G.; Persico, M. *Chem. Phys.* **1992**, *167*, 121.

(13) Balabanov, N. B.; Boggs, J. E. *J. Phys. Chem. A* **2000**, *104*, 1597.

(14) Van Der Sluys, L. S.; Eckert, J.; Eisenstein, O.; Hall, J. H.; Huffman, J. C.; Jackson, S. A.; Koetzle, T. F.; Kubas, G. J.; Vergamini, P. J.; Caulton, K. G. *J. Am. Chem. Soc.* **1990**, *112*, 4831.

(15) Bronger, W.; Sommer, T.; Auffermann, G.; Muller, P. *J. Alloys Compd.* **2002**, *330*, 536.

(16) Wang, X.; Andrews, L. *J. Phys. Chem. A* **2000**, *104*, 9892 (Ru + CO, $H_2$).

(17) For example:(a) Bautista, M.; Earl, K. A.; Morris, R. A.; Sella, A. *J. Am. Chem. Soc.* **1987**, *109*, 3780. (b) Hamilton, D. G.; Crabtree, R. H. *J. Am. Chem. Soc.* **1988**, *110*, 4126. (c) Jia, G.; Meek, D. W. *J. Am. Chem. Soc.* **1989**, *111*, 757.

(18) For example:(a) Arliguie, T.; Chaudret, B.; Morris, R. H.; Sella, A. *Inorg. Chem.* **1988**, *27*, 598. (b) Albeniz, M. J.; Buil, M. L.; Esteruelas, M. A.; Lopez, A. M.; Oro, L. A.; Zeier, B. *Organometallics* **1994**, *13*, 3746. (c) Bardajf, M.; Caminade, A.-M.; Majoral, J.-P.; Chaudret, B. *Organometallics* **1997**, *16*, 3489.

(19) Crabtree, R. H. *Chem. Rev.* **1985**, *85*, 245.

(20) (a) Alonso, D. A.; Brandt, P.; Nordin, S. J. M.; Andersson, P. G. *J. Am. Chem. Soc.* **1999**, *121*, 9580. (b) Jia, G.; Lau, C. P. *Coord. Chem. Rev.* **1999**, *192*, 83. (c) Older, C. M.; Stryker, J. M. *J. Am. Chem. Soc.* **2000**, *122*, 2784.

(21) (a) Bolano, T.; Castarlenas, R.; Esteruelas, M. A.; Onate, E. *J. Am. Chem. Soc.* **2007**, *129*, 8850. (b) Casey, C. P.; Singer, S. W.; Powell, D. R.; Hayashi, R. K.; Kavana, M. *J. Am. Chem. Soc.* **2001**, *123*, 1090.

(22) (a) Creutz, C.; Chou, M. H. *J. Am. Chem. Soc.* **2007**, *129*, 10108. (b) Hierso, J. C.; Amardeil, R.; Bentabet, E.; Broussier, R.; Gautheron, B.; Meunier, P.; Kalck, P. *Coord. Chem. Rev.* **2003**, *236*, 143.

(23) (a) Kubas, G. J. *Proc. Natl. Acad. Sci.U.S.A.* **2007**, *104*, 6901. (b) Lau, C. P.; Ng, S. M.; Jia, G.; Lin, Z. *Coord. Chem. Rev.* **2007**, *251*, 2223.

(24) Andrews, L.; Wang, X. *Science* **2003**, *299*, 2049 (Al + $H_2$).

(25) Wang, X.; Andrews, L. *J. Phys. Chem. A* **2003**, *107*, 570 (Cr+$H_2$).

(26) (a) Wang, X.; Andrews, L. *Angew. Chem., Int. Ed.* **2003**, *42*, 5201. (b) Wang, X.; Andrews, L.; Manceron, L.; Marsden, C. *J. Phys. Chem. A* **2003**, *107*, 8492 (Cu, Ag, Au + $H_2$). (c) Wang, X.; Andrews, L. *J. Am. Chem. Soc.* **2003**, *125*, 6581 (Pb, Sn +$H_2$).

(27) (a) Wang, X.; Andrews, L.; Infante, I.; Gagliardi, L. *J. Am. Chem. Soc.* **2008**, *130*, 1972 (W + $H_2$). (b) Wang, X.; Andrews, L.; Gagliardi, L. *J. Phys. Chem. A* **2008**, *112*, 1754 (Th + $H_2$).

(28) Wang, X.; Andrews, L. *Organometallics* **2008**, *27*, 4273. ($RuH_2(H_2)_4$ communication).

(29) (a) Andrews, L.; Citra, A. *Chem. Rev.* **2002**, *102*, 885, and references therein. (b) Andrews, L. *Chem. Soc. Rev.* **2004**, *33*, 123, and references therein.

(30) Frisch, M. J.; Trucks, G. W.; Schlegel, H. B.; Scuseria, G. E.; Robb, M. A.; Cheeseman, J. R.; Montgomery, J. A. Jr.; Vreven, T.; Kudin, K. N.; Burant, J. C.; Millam, J. M.; Iyengar, S. S.; Tomasi, J.; Barone, V.; Mennucci, B; Cossi, M.; Scalmani, G.; Rega, N.; Petersson, G. A.; Nakatsuji, H.; Hada, M.; Ehara, M.; Toyota, K.; Fukuda, R.; Hasegawa, J.; Ishida, M.; Nakajima, T.; Honda, Y.; Kitao, O.; Nakai, H.; Klene, M.; Li, X.; Knox, J. E.; Hratchian, H. P.; Cross, J. B.; Adamo, C.; Jaramillo, J.; Gomperts, R.; Stratmann, R. E.; Yazyev, O.; Austin, A. J.; Cammi, R.; Pomelli, C.; Ochterski, J. W.; Ayala, P. Y.; Morokuma, K.; Voth, G. A.; Salvador, P.; Dannenberg, J. J.; Zakrzewski, V. G.; Dapprich, S.; Daniels, A. D.; Strain, M. C.; Farkas, O.;. Malick, D. K; Rabuck, A. D.; Raghavachari, K.; Foresman, J. B.; Ortiz, J. V.; Cui, Q.; Baboul, A. G.; Clifford, S.; Cioslowski, J.; Stefanov, B. B.; Liu, G.; Liashenko, A.; Piskorz, P.; Komaromi, I.; Martin, R. L.; Fox, D. J.;. Keith, T.; Al-Laham, M. A; Peng, C. Y.; Nanayakkara, A.; Challacombe, M.; Gill, P. M. W.; Johnson, B.; Chen, W.; Wong, M. W.; Gonzalez, C.; Pople, J. A. *Gaussian 03, Revision B.04*; Gaussian, Inc.: Pittsburgh, PA, 2003. and references therein.

(31) Frisch, M. J.; Pople, J. A.; Binkley, J. S. *J. Chem. Phys.* **1984**, *80*, 3265.

(32) Andrae, D.; Haeussermann, U.; Dolg, M.; Stoll, H.; Preuss, H. *Theor. Chim. Acta* **1990**, *77*, 123.

(33) (a) Becke, A. D. *J. Chem. Phys.* **1993**, *98*, 5648. (b) Lee, C.; Yang, Y.; Parr, R. G. *Phys. Rev. B* **1988**, *37*, 785.

(34) Perdew, J. P.; Burke, K.; Wang, Y. *Phys. Rev. B* **1996**, *54*, 16533, and references therein.

(35) Andrews, L.; Chertihin, G. V.; Ricca, A.; Bauschlicher, C. W., Jr. *J. Am. Chem. Soc.* **1996**, *118*, 467 (Fe + $O_2$).

(36) Zhou, M.; Citra, A.; Liang, B.; Andrews, L. *J. Phys. Chem. A* **2000**, *104*, 3457 (Ru, Os + $O_2$).

(37) Chong, D. P.; Langhoff, S. R.; Bauschlicher, C. W., Jr.; Walch, S. P.; Partridge, H. *J. Chem. Phys.* **1986**, *85*, 2850.

(38) Langhoff, S. R.; Bauschlicher, C. W., Jr *J. Mol. Spectrosc.* **1990**, *141*, 243.

(39) Martini, H.; Marian, C. M.; Peric, M. *Mol. Phys.* **1998**, *95*, 27, and references therein.

(40) (a) Scott, A. P.; Radom, L. *J. Phys. Chem.* **1996**, *100*, 16502. (b) Andersson, M. P.; Uvdal, P. L. *J. Phys. Chem. A* **2005**, *109*, 3937.

(41) Balasubramanian, K.; Wang, J. Z. *J. Chem. Phys.* **1989**, *91*, 7761.

(42) (a) Andrews, L.; Manceron, L.; Alikhani, M. E.; Wang, X. *J. Am. Chem. Soc.* **2000**, *122*, 11011. (b) Andrews, L.; Wang, X.; Alikhani, M. E.; Manceron, L. *J. Phys. Chem. A* **2001**, *105*, 3052 (Pd + $H_2$).

(43) Wang, X.; Andrews, L. *J. Phys. Chem. A* **2002**, *106*, 3706 (Rh + $H_2$).

(44) Miller, A. E. S.; Feigerle, C. S.; Lineberger, W. C. *J. Chem. Phys.* **1986**, *84*, 4127.

(45) Duckett, S. B.; Mawby, R. J.; Partridge, M. G. *Chem. Commun.* **1996**, 383.

(46) See for example:(a) Morris, R. H.; Sawyer, J. F.; Shiralian, M.; Zubkowski, J. D. *J. Am. Chem. Soc.* **1985**, *107*, 5581. (b) Cappellani, E. P.; Drouin, S. D.; Jia, G.; Maltby, P. A.; Morris, R. H.; Schweitzer, C. T. *J. Am. Chem. Soc.* **1994**, *116*, 3375.

(47) (a) Wang, X.; Andrews, L. *J. Am. Chem. Soc.* **2002**, *124*, 7610. (b) Wang, X.; Andrews, L. *J. Phys. Chem. A* **2002**, *106*, 9213 (group 3 metals).

(48) Wang, X.; Andrews, L. *J. Phys. Chem. A* **2003**, *107*, 4081 (Mn, Re + $H_2$).

(49) Zhou, W.; Yildirim, T.; Durgun, E.; Ciraci, S. *Phys. Rev. B* **2007**, *76*, 085434.

JP806845H